Analyzing the impact of nonlinear density dependence on host-parasitoid dynamics

Laura Hu and Mia Prim

Department of Mathematics and Statistics, San Diego State University, San Diego, California 92182-7720, USA

Abstract

This study reviews a recent modification proposed to the Nicholson-Bailey model, which introduces a nonlinear dependence of parasitoid search efficiency on their density. This adjustment allows for more realistic population dynamics and the potential for local asymptotic stability. The model is further extended by incorporating spatial heterogeneity, which highlights the impact of spatially variable growth rates on host-parasitoid dynamics. This spatial variation disrupts uniform population behavior, leading to localized dynamics, spatially dependent coexistence mechanisms, and increased system complexity. The findings of this study provide a more robust and biologically relevant model for host-parasitoid interactions, contributing to the broader field of population biology and biological control.

Introduction

Predator-prey models are fundamental tools in ecological modeling, offering insights into population oscillations, stability, and the persistence of interacting species. Among these, the Nicholson-Bailey model has served as a cornerstone for studying host-parasitoid dynamics. Introduced by Nicholson and Bailey in 1935, this discrete-time model provides a foundational framework for exploring biological control, pest management, and other ecological phenomena.

Despite its historical importance, the Nicholson-Bailey model is inherently unstable, often predicting unbounded population oscillations that are rarely observed in real-world ecosystems. This limitation has motivated numerous extensions and modifications to incorporate more realistic ecological mechanisms and improve the model's stability and predictive power.

In this report, we present a modified Nicholson-Bailey model that incorporates nonlinear density dependence in the host population. By reducing parasitoid efficiency at higher host densities, this modification more accurately captures real-world host-parasitoid dynamics and mitigates the instability of the original model. Through analytical and numerical studies of equilibrium points and stability conditions, we demonstrate the potential for local asymptotic stability under specific scenarios.

To further enrich our analysis, we extend the model to include spatial heterogeneity, introducing variability in growth rates across a grid. This spatial element disrupts the system's symmetry, leading to localized dynamics where host and parasitoid populations evolve differently across regions. Our findings reveal that spatial extensions can uncover mechanisms for coexistence and stability absent in non-spatial models, such as the creation of refuges and patchy population distributions.

Through these combined approaches, we deepen the understanding of host-parasitoid interactions, explore the interplay between local and spatial dynamics, and discuss implications for ecological modeling.

Model Formulation

Parasitoids are insect species whose larvae develop by feeding on the bodies of other arthropods, ultimately killing the host. After the larvae emerge, they develop into free-living adults, continuing the cycle. The study of population dynamics in biological control has evolved over many decades, with host-parasitoid models being favored due to three key assumptions [1]:

1. Hosts that are parasitized will give rise to the second generation of parasitoids.

2. Hosts that have not been parasitized will keep reproducing.

3. The proportion of parasitized hosts depends on the rate of encounters between hosts and parasitoids.

This modeling tradition, initiated mainly by entomologists studying insect hosts and their parasitoids, assumes discrete and synchronized generations [1]. In contrast to the continuous-time Lotka–Volterra models, which assume overlapping generations and continuous birth-death processes, the discrete-generation framework is more suitable for many host-parasitoid systems as it introduces a one-generation time lag between the act of parasitism and the resulting change in host populations [1].

The typical framework for discrete-generation host-parasitoid models is given by

$$H_{t+1} = rH_t f(H_t, P_t), \tag{1}$$
$$P_{t+1} = cH_t \left(1 - f(H_t, P_t)\right), \tag{2}$$

where H and P represent the population sizes of susceptible hosts and searching adult female parasitoids, respectively, in successive generations t and $t + 1$. Here, rH_t is the per capita net growth rate of the host population in the absence of the parasitoids, $f(H_t, P_t)$ is the fractional functional response of hosts that avoid parasitoid attacks, and c is the average number of viable eggs laid by a parasitoid on a single host [1, 2].

The most influential discrete-time model was developed by A.J. Nicholson and V.A. Bailey in 1935, using a Holling

type I linear functional response [1, 2]. They assumed parasitoid attacks occured randomly among hosts, with the average attack rate determined entirely by the number of parasitoids, rather than by egg limitation. The probability of a host encountering a parasitoid follows a Poisson distribution, where the number of parasitoids determines the likelihood of contact, and a host becomes infested after its first encounter with a parasitoid [2, 3]. The probability $p(r)$ of r encounters, given an average number of encounters μ_t, is expressed as

$$p(r) = \frac{e^{-\mu}\mu^r}{r!},$$

where $\mu = aP_t$ represents the expected number of encounters and a denotes the parasitoid's search efficiency. The fraction of hosts not parasitized, $f(H_t, P_t)$, corresponds to the probability of zero encounters, $p(0)$, which is expressed as $f(H_t, P_t) = f(P_t) = e^{-aP_t}$.

Substituting the derived functional response into the general framework (1)-(2) yields the search-independent and randomly-selected Nicholson-Bailey model:

$$H_{t+1} = rH_t e^{-aP_t}, \tag{3}$$
$$P_{t+1} = H_t \left(1 - e^{-aP_t}\right). \tag{4}$$

This model implicitly assumes that parameter c in (2) is 1, meaning each attacked host results in exactly one parasitoid female, which is suitable only for solitary parasitoids in which the male sex is absent [2].

While this model captures the basic dynamics of host-parasitoid interactions, it predicts intrinsic instability, with small perturbations leading to unbounded oscillations – an outcome biologically unrealistic in most cases [2]. To address this, M.N. Queresh et al. (2014) proposed a modification in which the search area per parasitoid is inversely proportional to $\sqrt{P_t}$ [4]. This adjustment yields the following equations:

$$H_{t+1} = rH_t e^{-a\sqrt{P_t}}, \tag{5}$$
$$P_{t+1} = H_t \left(1 - e^{-a\sqrt{P_t}}\right), \tag{6}$$

which reflects reduced parasitoid efficiency at higher densities. This modification introduces the potential for local asymptotic stability, which the original model lacked. Throughout this study, it is assumed that $r > 1$, reflecting the condition that the host reproduction rate must exceed replacement levels for the population to persist.

Analysis

The steady state populations, denoted as (H^*, P^*), are the solutions that satisfy $H_{t+1} = H$ and $P_{t+1} = P$. Solving the system (5)-(6) under these conditions yields two equilibria. The first is the trivial equilibrium $(H_1^*, P_1^*) = (0,0)$, and the second is a coexistence equilibrium, given by

$$(H_2^*, P_2^*) = \left(\frac{r}{r-1}\left(\frac{1}{a}\ln r\right)^2, \left(\frac{1}{a}\ln r\right)^2\right). \tag{7}$$

The local stability of these equilibria is determined by analyzing the Jacobian matrix of the system (5)-(6), which is given by

$$J_{(H,P)} = \begin{pmatrix} re^{-a\sqrt{P}} & \frac{-arHe^{-a\sqrt{P}}}{2\sqrt{P}} \\ 1 - e^{-a\sqrt{P}} & \frac{aHe^{-a\sqrt{P}}}{2\sqrt{P}} \end{pmatrix}.$$

Evaluated at the origin, the Jacobian has eigenvalues $\lambda = r$ and $\lambda = 0$. Since $r > 1$ by assumption, the trivial equilibrium is always a saddle point, with the unstable eigenvalue $\lambda = r$ causing divergence along one direction. At the coexistence equilibrium, the Jacobian simplifies to

$$J_{(H_2^*, P_2^*)} = \begin{pmatrix} 1 & -\frac{r\ln(r)}{2(r-1)} \\ \frac{r-1}{r} & \frac{\ln(r)}{2(r-1)} \end{pmatrix}.$$

The characteristic polynomial of $J_{(H_2^*, P_2^*)}$ is

$$P(\lambda) = \lambda^2 - \left(1 + \frac{\ln r}{2(r-1)}\right)\lambda + \frac{r\ln r}{2(r-1)}.$$

Letting $\beta = 1 + \ln(r)/2(r-1)$ and $\varphi = r\ln(r)/2(r-1)$, the eigenvalues are determined as

$$\lambda = \frac{\beta^2 \pm \sqrt{\beta^2 - 4\varphi}}{2}.$$

For the coexistence equilibrium to be stable, the eigenvalues must satisfy $|\lambda| < 1$. To analyze this, observe that $|\beta| < 1 + \varphi$. By rewriting this bound, we have

$$-1 - \varphi < \beta < 1 + \varphi.$$

It follows that $|\beta| < 1 + \varphi < 2$. As $1 + \varphi < 2$ holds, we can equivalently restate the stability condition as

$$\Phi(r) = \ln r - 2r + 2 < 0.$$

Numerical evaluation of $\Phi(r)$ via a root-finding scheme shows that the critical reproductive rate is approximately $r_c \approx 4.92155363$. This indicates that the positive equilibrium in (7) is locally stable only if $1 < r < r_c$, beyond which the system becomes unstable.

To better understand the system's behavior across varying growth rates r, we illustrate its dynamics through a combination of time series plots and phase-space trajectories, as shown in Figure 1. The densely-filled scatter plots compare the trajectories for different values of r, highlighting convergence, periodic and quasi-periodic oscillations, and more complex patterns. The results confirm that stable coexistence occurs only when $r \in (1, r_c)$. For simplicity and without loss of generality, we fix $a = 1$ for the remainder of the analysis, as this parameter is merely a scaling factor that influences interaction rates between species and does not qualitatively alter the behavior.

Starting from initial conditions near the coexistence equilibrium, the trajectories exhibit diverse dynamics depending on the growth rate r: convergence to stability for $r < r_c$,
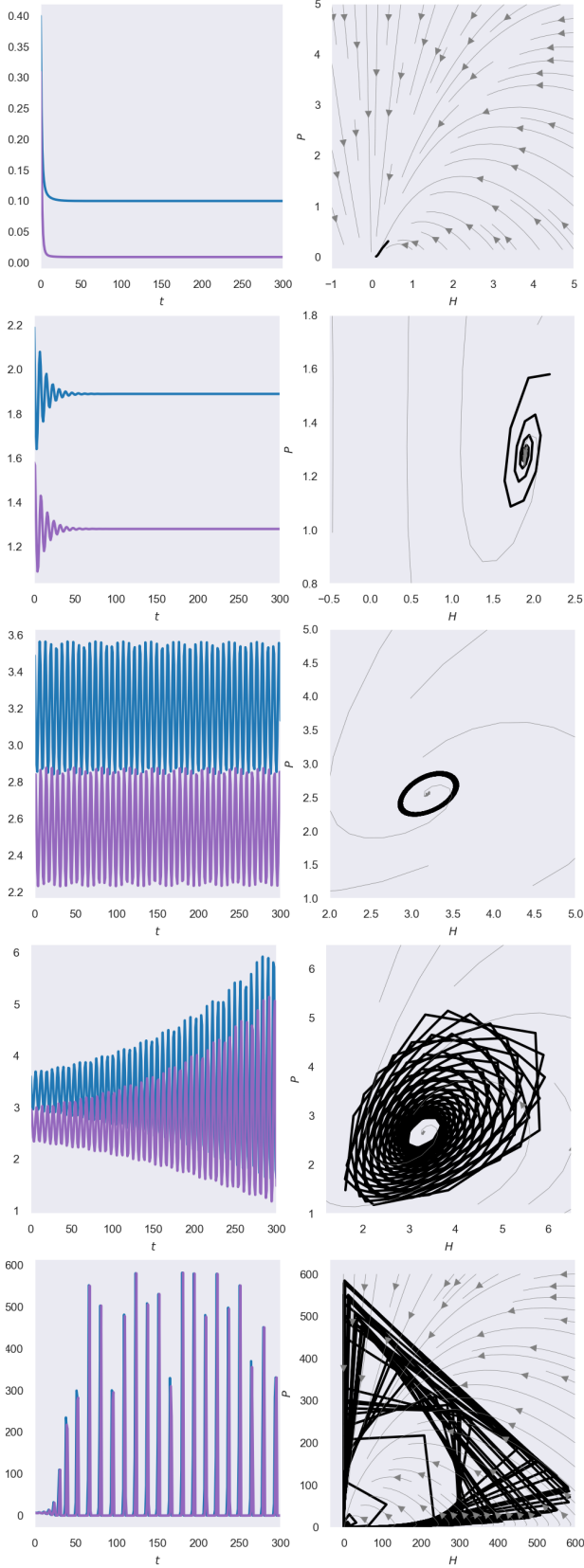
Figure 1: Time series of H_t (blue) and P_t (purple), with corresponding phase-space portraits directly to the right. From top to bottom: $r = 1.1, 3.1, r_c, 5.1, 12$ with $(H_0, P_0) = (H_2^* + 0.3, P_2^* + 0.3)$.
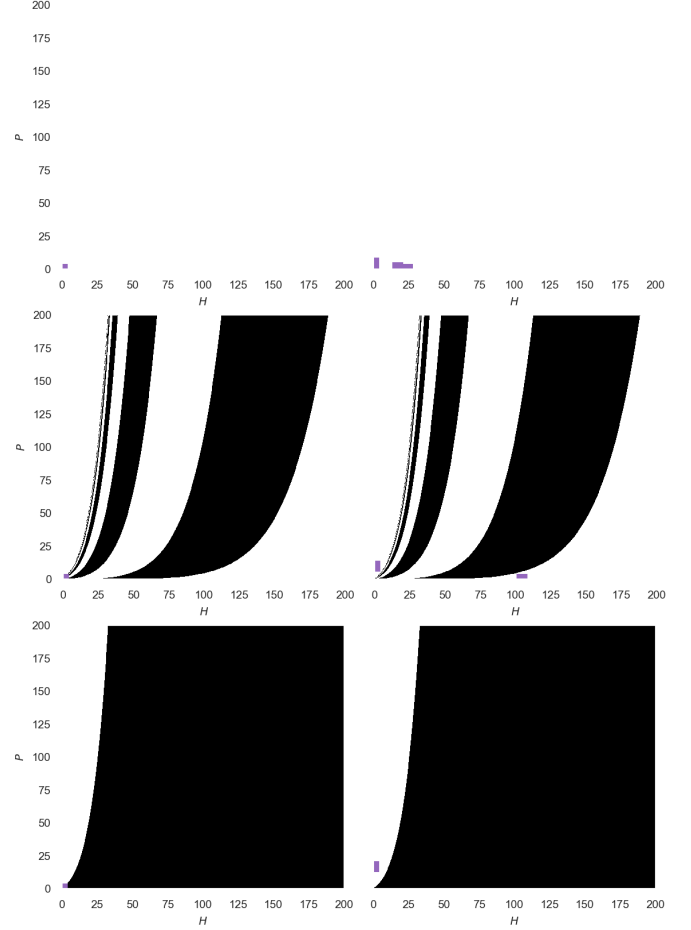

Figure 2: Basin of attraction (white) for (top) $r = 10.29$ and (bottom) $r = 17.2$. Purple crosses denote (left) period-1 sinks at the origin and (right) period-2 sinks. As r increases, the basin of infinity (black) dominates the grid.

periodic oscillations at $r = r_c$, and quasi-periodic behavior for $r > r_c$, with trajectories densely filling a toroidal structure, indicative of complex dynamics.

A deeper exploration of phase-space behavior reveals the influence of saddle points. Although saddles, as well as sources, are both unstable fixed points, saddles exhibit a unique property: not all nearby initial conditions diverge away [5]. Instead, certain trajectories converge to the saddle, forming its stable manifold. In this system, the stable manifold corresponds to the $P-$axis in the first quadrant. This boundary plays a critical role in determining the fate of nearby trajectories, separating regions that diverge from those that converge [5]. Although saddles are not attractors, their influence on the overall dynamics is decisive.

As r increases even further beyond r_c, the dynamics become more intricate. Figure 2 illustrates the outcomes of iterating the map for various initial conditions distributed across a grid of 1000×1000 points within the region $[0, 200] \times [0, 200]$. All initial values that diverge to infinity are marked in black, while those converging to a periodic orbit are shown in white. The purple crosses indi-

cate the location of period−n sinks, which attract white initial values. Interestingly for $a = 10.24$, the basin boundary exhibits fractal-like behavior, whereas for $r = 12.1$, it smoothens out into a regular curve. Despite the intricate dynamics, numerical analysis does not reveal the presence of a chaotic attractor, limiting the applicability of the map for calculating fractal and correlation dimensions.

These basin structures hint at underlying transitions in the system's behavior as r increases. To explore these transitions more systematically, we turn to the bifurcation diagram in Figure 3, which traces the evolution of the host population as it passes through r_c. At this critical point, a Neimark-Sacker bifurcation occurs, marked by the emergence of complex conjugate eigenvalues with unit modulus [6]. This bifurcation gives rise to the closed invariant curve previously illustrated in the phase space.
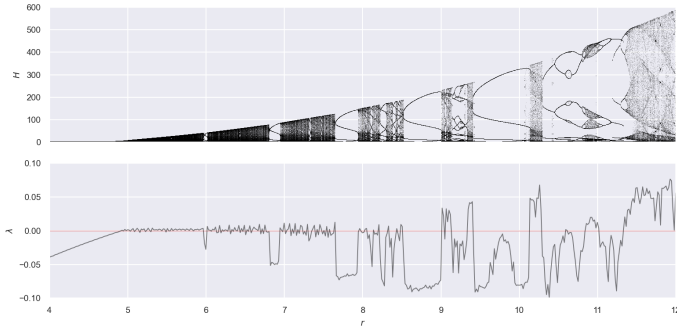

Figure 3: Transition of H through r_c where it undergoes a Neimark-Sacker bifurcation, followed by period-doubling cascades, eventually leading to chaos.

Beyond the Neimark-Sacker bifurcation, further increases in r reveal additional structural changes in the system. Period-doubling bifurcations appear, potentially signaling a flip bifurcation, and pave the way for chaotic behavior. This progression is further supported by Lyapunov exponent computations using the Gram-Schmidt QR factorization method, which quantify trajectory sensitivity to initial conditions. Oscillations of the stretching exponent around zero align with the quasi-periodic regions observed in phase-space diagrams. While the bifurcation patterns of the parasitoid population are not explicitly shown, they closely parallel those of the host population and can be similarly analyzed.

Incorporation of Spatial Dynamics

In further analyzing this model, we extend the simple Nicholson-Bailey framework to incorporate spatial dynamics. Although host-parasitoid interactions often exhibit strong fluctuations from year to year, as seen in the Nicholson-Bailey model, they rarely lead to the complete extinction of either species. One key factor neglected in the basic Nicholson-Bailey model is spatial structure. While populations can sometimes be considered well-mixed, this assumption is often unrealistic, as both species' interactions

and offspring dispersal tend to be localized [7]. In ecological systems, spatial heterogeneity plays a fundamental role in population dynamics, with dispersal and localized interactions generating patterns such as patchiness, coexistence, and even chaotic spatial structures—features absent in non-spatial models. By incorporating spatial dynamics, we can explore how dispersal influences stability and coexistence.

We consider the approach taken by [7], where the Nicholson-Bailey dynamics occur on a spatial grid. At each site (i, j), the dynamics are given by the modified Nicholson-Bailey model (5)-(6) from the previous section, with the addition of host and parasitoid dispersal to immediately neighboring sites. The dispersal rates for hosts and parasitoids are denoted by d_h and d_p, respectively, and the spatially adjusted populations are given by

$$H_{ij}(t+1) = RH_{ij}^*(t)e^{-a\sqrt{P_{ij}^*(t)}}, \qquad (8)$$

$$P_{ij}(t+1) = cH_{ij}^*(t)\left(1 - e^{-a\sqrt{P_{ij}^*(t)}}\right), \qquad (9)$$

where the time dependence is no longer indicated by a subscript. The dispersal-adjusted populations are

$$H_{ij}^* = (1 - d_h)H_{ij} + \frac{d_h}{8}\sum_{kl} H_{kl}(t),$$

$$P_{ij}^* = (1 - d_p)P_{ij} + \frac{d_p}{8}\sum_{kl} P_{kl}(t),$$

with the sum being over all eight neighboring sites $(i-1, j-1), \ldots, (i+1, j+1)$. The host population is initialized to 1 at every site, while the parasitoid population starts at 0 except for the central site, where it is initialized to 1. We also apply periodic boundary conditions, ensuring that the grid is toroidal in the sense that moving past one edge of the 100×100 lattice results in reappearing on the opposite side.

For $r > r_c$, the host-parasitoid populations exhibit patchiness with a symmetrical Turing-like spatial distribution. This is a significant departure from the non-spatial model, which predicts instability and chaos for high reproductive rates. Dispersal introduces spatial refuges where hosts can persist despite parasitoid pressure, enabling coexistence. These patterns emerge from a balance between local extinction events and recolonization from neighboring patches.

As seen in Figure 4, lower dispersal rates lead to localized populations around their initial positions. Hosts far from parasitoids experience less pressure due to the slow spread of parasitoids. The slow dispersal of parasitoids results in coexistence across many small, isolated patches with high and low population densities. In contrast, higher dispersal rates accelerate population mixing, leading to more synchronized dynamics across the grid. Hosts become more uniformly impacted by parasitoids, with synchronized oscillations across the grid as dispersal connects distant areas rapidly, leaving hosts struggling to escape parasitoid pressure.
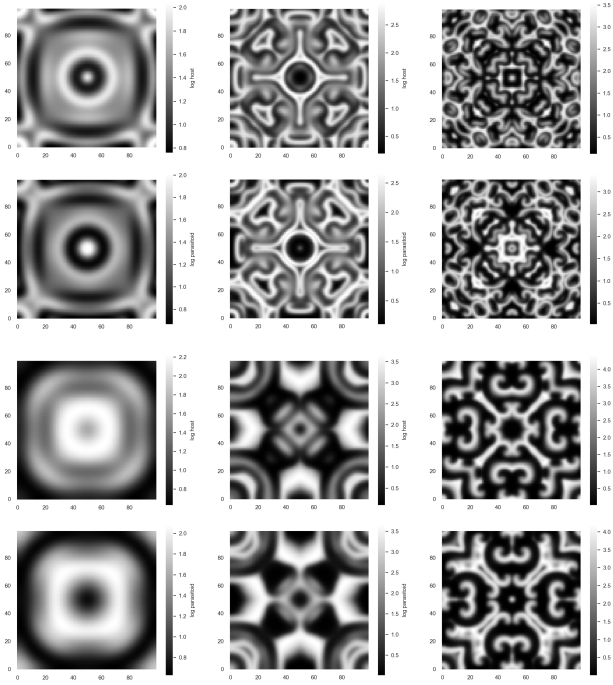
Figure 4: Spatial model with r constant. Host and parasitoid population densities are shown on a logarithmic scale for $d_p = d_h = 0.1$ (first and two rows: $r = 5.1, 5.5, 6.1$) and $d_p = d_h = 0.5$ (bottom two rows: $r = 5.1, 6.1, 8.1$).
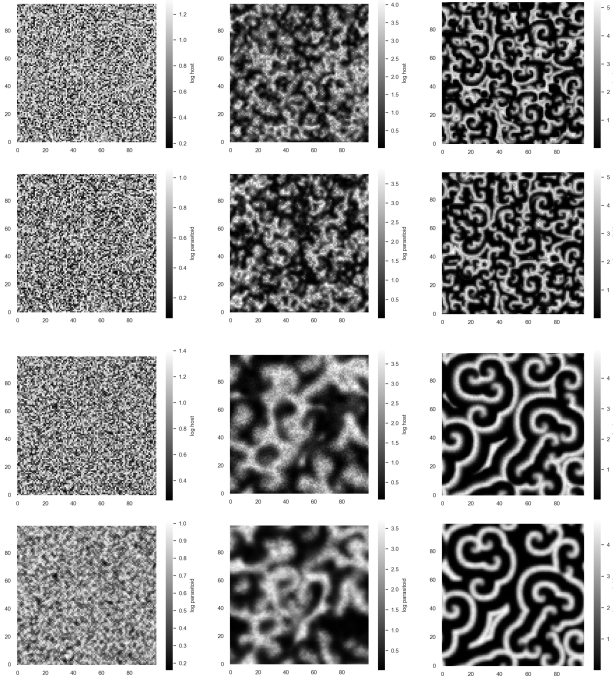

Figure 5: Introduction of a spatial heterogeneity in the system with randomly distributed r. Hosts and parasitoid population densities are shown for $d_p = d_h = 0.1$ (first two rows) and $d_p = d_h = 0.5$ (bottom two rows), for $r \in (1, 4), (4, 8), (8, 12)$.

The introduction of spatial variability in the interaction parameter r disrupts the symmetry of the system, as illustrated in Figure 5. By treating r as a random variable with uniformly distributed values, the growth rate of the host population H_t becomes heterogeneous across the grid. This variability leads to regions where host growth is accelerated due to higher values of r, resulting in localized hotspots of increased population density. Conversely, areas with lower values of r experience slower growth and reduced host densities, contributing to a more complex and non-uniform overall population distribution.

This spatial variability in r introduces anisotropic effects, where the evolution of populations is influenced by both direction and local conditions. The dynamics of the host population are shaped not only by the intrinsic growth rate rH_t but also by interactions with the parasitoid population P_t. Consequently, regions with elevated r values, which correspond to enhanced host growth, may sustain larger parasitoid populations. In contrast, areas with lower r values tend to have lower host densities, leading to a corresponding decline in parasitoid populations. This spatial dependence creates feedback loops between host and parasitoid populations, resulting in varying predation pressures across the grid and further breaking the system's symmetry.

Moreover, the randomness in r gives rise to localized dynamics, resulting in a patchy distribution of host and parasitoid populations. This patchiness can give rise to intricate spatial structures, characterized by clusters of high-density regions interspersed with areas of low density. The behavior of the system becomes contingent on local values of r, which may lead to differing stability characteristics throughout the grid. In regions with higher r, the system tends to achieve elevated stable population levels, while areas with lower r are more susceptible to extinction or maintain lower stable populations.

When visualized, the populations no longer display the uniformity characteristic of the symmetric case. Instead, both host and parasitoid populations exhibit significant spatial variation, with some areas showing higher concentrations and others lower. This broken symmetry is reflected in the observed patterns, as population dynamics increasingly depend on local variations in r. In regions where r is lower, Turing instability manifests, leading to high instability in host and parasitoid populations across two-dimensional space [8]. Conversely, areas with higher r values, particularly when coupled with elevated diffusion rates, tend to exhibit stability. Low diffusion rates result in localized, high-variance patterns, while higher diffusion rates promote larger-scale, smoother population structures. The randomness in r adds an additional layer of complexity, producing a spectrum of spatial patterns that range from chaotic-like configurations to more ordered arrangements.

Spatial extensions like these reveal mechanisms for coexistence that are not evident in non-spatial models. The feedback between host and parasitoid populations becomes more intricate as spatial heterogeneity promotes local

refuges for hosts, allowing them to evade complete extinction in certain regions even under strong parasitoid pressure. This highlights the stabilizing role of spatial structure and dispersal in ecological models, where the movement of individuals between regions with different population densities can foster coexistence and persistence. By incorporating such spatial features, we gain a more realistic understanding of how populations might survive and interact in fragmented habitats, where the dynamics of local areas can significantly differ from the global average.

Conclusion

The Modified Nicholson-Bailey Model introduces nonlinear density dependence to address the biological complexities of host-parasitoid interactions. By introducing a reduced parasitoid efficiency at higher densities, the modified model provides a more realistic representation of these interactions compared to traditional models. Our analysis of equilibrium points through the linearization of the system indicates that under certain conditions, the system can achieve local asymptotic stability, offering a foundation for understanding the long-term dynamics of host-parasitoid populations.

In addition to the core dynamics, we explored the role of spatial heterogeneity in shaping population interactions. The incorporation of spatial structure allows for a more detailed understanding of how local variations in growth rates, due to a randomly distributed interaction parameter r, affect the population dynamics. By disrupting the symmetry of the system, this spatial variability introduces localized differences in host and parasitoid growth, leading to more complex and spatially dependent dynamics. The system's behavior, including the potential for localized extinction events and varying population densities, underscores the importance of considering spatial factors in ecological modeling.

Looking ahead, future work will focus on extending our analysis through further numerical simulations to examine the correlation between dynamics at two distinct locations as a function of their distance. This will deepen our understanding of spatial interactions and their implications for the stability and persistence of host-parasitoid populations.

References

[1] Hassell, M. (2001). Host-parasitoid population dynamics. *Journal of Animal Ecology*, 69(4): 543-566.

[2] Mills, N., et al. (1996). Modelling the biological control of insect pests: a review of host-parasitoid models. *Ecological Modelling*, 92(2): 121-143.

[3] Jamieson, W., et al. (2018). Global behavior for the classical Nicholson–Bailey model. *Journal of Mathematical Analysis and Applications*, 461(1): 492-499.

[4] Qureshi, M., et al. (2014). Asymptotic behavior of a Nicholson-Bailey model. *Advances in Difference Equations volume*, 62.

[5] Aligood, K., et al. (2000). CHAOS: An Introduction to Dynamical Systems. *Springer.*

[6] Din, Q., et al. (2021) Modification of Nicholson–Bailey model under refuge effects with stability, bifurcation, and chaos control. *Journal of Vibration and Controls*, 28(23-24): 3524–3538.

[7] Bonhoeffer, S. Nicholson-Bailey Model. *BioSym Lab.*

[8] Zhang, X., et al. (2023). The Diffusion-Driven Instability for a General Time-Space Discrete Host-Parasitoid Model. *Discrete Dynamics in Nature and Society*, 2023(1).